eROSITA

P. Predehl[1], G Hasinger[1], H. Böhringer[1], U. Briel[1], H. Brunner[1], E. Churazov[7], M. Freyberg[1], P. Friedrich[1], E. Kendziorra[3], D. Lutz[1], N. Meidinger[1], M.Pavlinsky[6], E. Pfeffermann[1], A. Santangelo[3], J. Schmitt[4], P. Schuecker[1], A. Schwope[2], M. Steinmetz[2], L. Strüder[1], R. Sunyaev,[6,7], J. Wilms[5]

[1] Max-Planck-Institut für extraterrestrische Physik, Garching (MPE), Germany
[2] Astrophysikalisches Institut Potsdam (AIP), Germany
[3] Institut für Astronomie und Astrophysik der Universität Tübingen (IAAT), Germany
[4] Universität Hamburg, Hamburger Sternwarte, Germany
[5] Dr. Remeis-Sternwarte, Astronomisches Institut der Universität Erlangen-Nürnberg, Germany
[6] Space Research Institute, IKI, Moskau, Russia
7 Max-Planck-Institut für Astrophysik, Garching, Germany

ABSTRACT

eROSITA (extended ROentgen Survey with an Imaging Telescope Array) will be one out of three main instruments on the Russian new Spectrum-RG mission which will be launched in the timeframe 2010-2011 into an equatorial Low Earth Orbit. The other two instruments are the wide field X-ray monitor Lobster (Leicester University, UK) and ART (IKI, Russia), an X-ray concentrator based on a Kumakhov optics. eROSITA consists of seven Wolter-I telescope modules similar to the German mission ABRIXAS which failed in 1999 and ROSITA, a telescope which was planned to be installed on the International Space Station ISS. Unlike these, the eROSITA telescope modules will be extended by adding another 27 mirror shells to the already existing ABRIXAS design. This will increase the effective area by a factor of ~5 at low energies. The additional shells do not contribute to the area at higher energies (> 5 keV) due to the relative large grazing angles. Here we stay with the old ABRIXAS/ROSITA effective area. However, the primary scientific goal has changed since ABRIXAS: we are now aiming primarily for the detection of 50-100 thousands Clusters of Galaxies up to redshifts z > 1 in order to study the large scale structure in the Universe and test cosmological models including the Dark Energy, which was not yet known at ABRIXAS times. For the detection of clusters, a large effective area is needed at low (< 2 kev) energies. The mission scenario comprises a wide survey of the complete extragalactic area and a deep survey in the neighborhood of the Galactic Poles. Both are accomplished by an all-sky survey with a tilt of the rotation axis in order to shift the deepest exposures away from the ecliptic poles towards the galactic poles.

Keywords: x-ray astronomy, all-sky survey, x-ray telescopes

1. INTRODUCTION

The heritage of eROSITA is a long series of scientific and technological developments starting with the extremely successful ROSAT mission which performed the first all-sky survey with an imaging X-ray telescope. Among other achievements, the cosmic X-ray background could be resolved almost completely into discrete sources, primarily black holes in the nuclei of active galaxies (AGN). The comparison of nearby and far distant (i.e., early) AGN allows to study the growth and the cosmological evolution of black holes. However, it became clear that ROSAT, with its "soft" telescope and therefore only narrow spectral bandwidth, could detect only a small fraction of the entire population of accreting black holes. The explanation of the rather hard spectrum with its maximum at ~ 30keV is that most of the AGN are obscured by a large amount of gas and dust in the centers of their host galaxies. Chandra and XMM have a spectral range up to ~ 10keV, substantially wider than that of ROSAT. However, these observatories can perform only pointed observations and cover only a small portion of the sky. The basic idea of ABRIXAS and ROSITA (Predehl et al. 1999, 2003) was therefore to extend the ROSAT all-sky survey towards higher energies. ABRIXAS failed unfortunately

shortly after launch due to a malfunction in the power system. ROSITA underwent several design studies and was technically verified. But the ISS turned out to be not suitable: according to the overall schedule, ROSITA had a launch date not before 2011, one year after the planned end of Shuttle flights. In addition, we have made an exposure experiment on the Russian module of the ISS for two years which showed that the (dirty) environment of the ISS is unsuitable for an X-ray instrument (Friedrich et al., 2005). Parallel to these activities, the development of new detector types based on the successful pn-CCD camera onboard XMM-Newton had been started.

Around 2000 new observational data have led to spectacular detections, which independently from each other convinced most astronomers of the existence of a "Dark Energy" which dominates all other forms of energy but acts on scales comparable with the size of the Universe. Therefore very large surveys became important for detailed studies. Clusters of galaxies are excellently suited for this kind of precision cosmology. Since they are easily detectable in X-rays, several proposals for projects of cluster surveys were made. In 2003 we participated in a proposal to NASA for the SMEX-mission DUO ("Dark Universe Observatory") based on a slight modification of the ROSITA telescope. Main task of DUO would have been the detection of ~ 10,000 clusters of galaxies. Meanwhile the fabrication of the new CCD in our semiconductor lab had been finished. However, NASA was not able to support DUO beyond its Phase-A study. A "White Paper", initialized by NSF, DOE, and NASA on the future of Dark Energy research showed in 2005 that within technical feasibility, the detection of 100,000 clusters is possible. Such a number is needed for a precision measurement of the equation of state, and particularly for the measurement of "baryonic acoustic oscillations" in the power density spectrum of galaxy clusters. These oscillations have been detected for the first time in 2005 and would allow the model-free determination of the cosmological parameters.

In order to meet these requirements, the existing ABRIXAS design of the mirror modules had to be extended by adding 27 (outer) shells, thereby increasing the collecting power at low energies by a factor of five. The quality of the outer shells has to be better than those of ABRIXAS: in order to distinguish clusters from point sources at $z = 1$, an angular on-axis resolution of the mirrors < 15 arcsec is needed. eROSITA benefits from the past development: we constantly continued the development of pn-CCD detectors; the eROSITA prototype is already working, and we are building the engineering model now. We have re-started the mirror production at the company Carl Zeiss, the preferred mirror producer also for eROSITA. Within the framework of several industrial studies we have investigated all the mechanical and thermal aspects of such a large X-ray survey mission.

2. INSTRUMENTAL CONCEPT

2.1 Spectrum-RG mission

Spectrum-RG is a medium size satellite which will be launched in the timeframe 2010-2011 into a 600km equatorial orbit with a Soyuz-2 rocket from Kourou. Apart from eROSITA, the payload comprises a wide field X-ray monitor (Lobster), supplied by an UK-led consortium, ART-XC, an X-ray concentrator based on a Kumakhov optics (supplied by IKI in Moscow), and a Gamma Ray Burst monitor built by a Russian consortium (Fig. 1). The equatorial low Earth orbit was chosen because of its low particle background. Since we want to study, among other targets, low surface brightness diffuse emission, we need to keep the intrinsic background as low as possible. For details see Pavlinsky et al. (2006).

2.2 eROSITA X-ray optics

The mirror replication technique was developed for XMM-Newton (an ESA Cornerstone Mission launched in 1999) and has then been applied to ABRIXAS, which had scaled the XMM telescopes down by a factor of about 4. The ABRIXAS optical design and manufacturing process are adopted for eROSITA partially because the focal length and the inner 27 mirror shells are kept the same. The mirror system consists of 7 mirror modules with 54 mirror shells each and a baffle in front of each module. Unlike on ABRIXAS, the seven optical axes are co-aligned (Fig. 2). Compared to a large single mirror system, the advantages of a multiple mirror system are: shorter focal length (reduced instrumental background), smaller mirror shells (easier to handle), and reduced pileup when observing bright sources. This configuration allows a more compact telescope and multiple but identical cameras which automatically provides a 7-fold of redundancy.

The mirror shells are manufactured by replication from super-polished mandrels. The reflective layers of gold copy the surface of the mandrel to get the required X-ray optical quality. The carrier material of the reflecting surface is electroformed nickel. The wall thickness of the mirror shells varies between 0.25 and 0.9 mm. All shells are adjusted and bonded to a supporting spider wheel. The capabilities of the X-ray mirror system are described by effective area,

vignetting function, and PSF. Since the entire FOV is used for the surveys, the measure for sensitivity is the product of the FOV-averaged effective area and the solid angle of the FOV ("grasp"). The characteristics are described in Table 1.

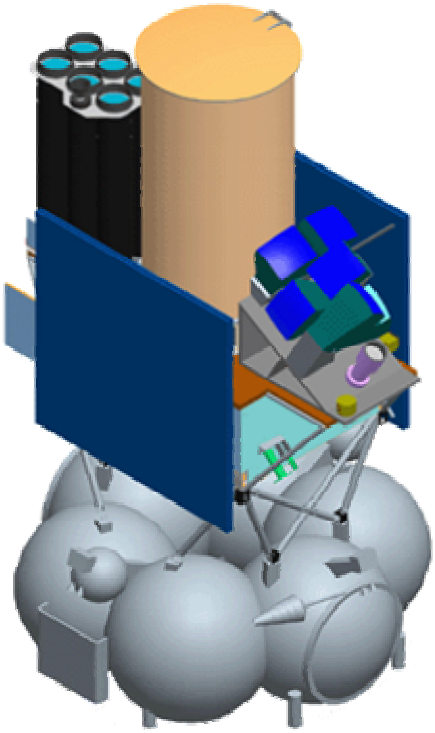

Fig. 1: Spectrum-RG in launch configuration, Yamal platform on Fregat-booster and the three instruments ART-XC, eROSITA and Lobster (left to right).

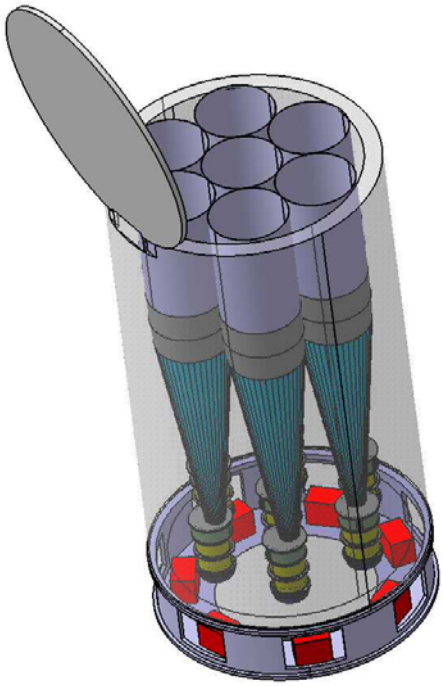

Fig. 2: The seven mirror modules with the baffles in front and the seven cameras at the rear end of the optical bench. Total length of the telescope is ~2,600mm, the diameter is ~1,300mm.

Table 1: Telescope parameters

mirror modules	7
mirror shells per module	54
energy range	0,2 < E < 12 keV
angular resolution	< 15'' on-axis
outer diameter	358 mm
inner diameter	76 mm
length of shells	300 mm

grazing angles	16' < α < 96'
wall thickess	0,2 – 0,9 mm
microroughness	< 0,5 nm RMS
mirror coating	Au (> 50 nm)
focal length	1600 mm
weight of mirror module	~ 57 kg
material of shell	Nickel

A stray light model optical system was developed including telescope baffles and the 10 nm aluminium blocking filter on the CCD. The worst case analysis indicated the visible photon background was 1×10^{-2} photons/s/pixel. This provides a margin of 5×10^{4} during the worst case observations in a direction only 15 degrees to the illuminated Earth limb. Scattered light due to solar illumination of the baffle interior was significantly lower. Less than about 180 mm of the outer part of the baffle is illuminated by the Sun in the worst case (60° to the telescope axis). The baffle tubes are thermally isolated from the temperature controlled mirror modules by GFRP isolations, preventing distortion from solar heating. An additional X-ray aperture stop (sieve plate system) will reduce the amount of single reflections from the rear end of the hyperboloid, if a bright source is just outside the field of view. The mirror system must be maintained at 20 ±2 °C during operation to avoid deformation and image degradation.

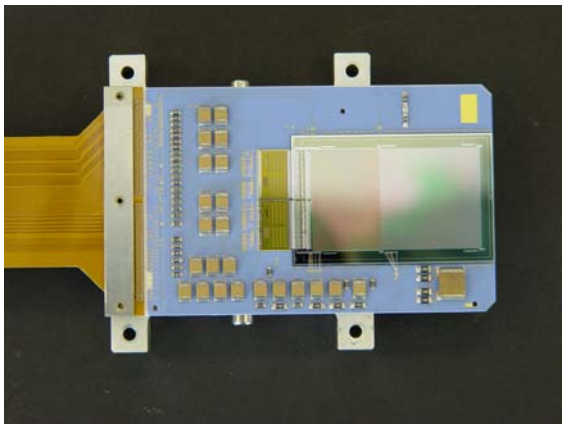

Fig. 3: eROSITA CCD-Module. The CCD with its image area (2×2 cm^2) and the slightly smaller frame store area (left) is connected via 256 bond wires with the two CAMEX read out chips. They are mounted, together with the (passive) front end electronics, on a ceramic printed circuit board (blue). The flexlead on the left connects the CCD-Module with the experiment electronics.

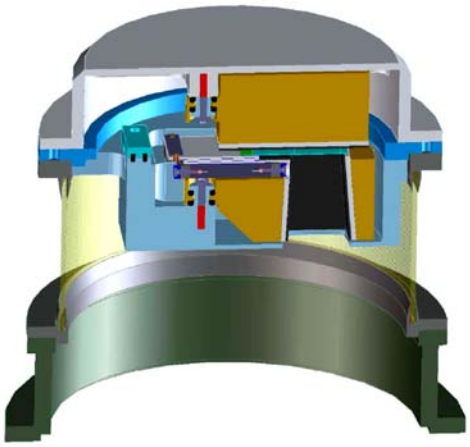

Fig. 4: Schematic representation of the camera housing with the cold plate (blue), CCD (green), and the copper radiation shield (brown). The light-green cylinder (GFRP) isolates thermally the cold part of the camera from the camera flange (dark-green).

2.3 eROSITA Camera

The pn-CCD camera onboard XMM-Newton (Pfeffermann et al. 2003) works without reduction of its performance since more than six years. During the recent years we have further improved the concept (Meidinger et al. 2006):

- The CCD has been extended by a frame store area which allows the fast shift from the image area in order to reduce so called out-of-time events, photons which are recorded during readout.
- The pixel size has been reduced to 75µm which fits better to the resolution of the eROSITA telescope.
- The use of 6inch silicon wafers with 450µm thickness gives a higher quantum efficiency at higher energies.
- The low energy response and energy resolution could be improved by a modification of the processing. At the same time, the operating temperature can be now as high as -60°C (XMM-Newton: -90°C).

Each of the seven mirror modules has its own camera in its focus, each equipped with a CCD-module and a processing electronics providing a 7-fold redundancy. The eROSITA-CCD has 256 × 256 pixels or a sensitive area of 19.2mm × 19.2mm, respectively, which corresponds to a field of view of 41.3 × 41.3 $arcsec^2$. The 256 channels are read out in parallel by two modified CAMEX-ICs (Fig. 3). The nominal integration time for eROSITA will be 50msec. The integrated image can be shifted into the frame store area by less than 100µsec before it is read out within about 5msec. CCD together with the two CAMEX and the (passive) front-end electronics are integrated on a ceramic printed board (= CCD-module) and is connected to the "outer world" by a flexlead. A flight-batch of more than 70 CCDs has been already fabricated. The CCD-module is already designed, fabricated, tested, and qualified (thermal vacuum, vibration). A prototype of the eROSITA camera is going to be installed in the PANTER X-ray test facility as a new "working horse".

The design of the camera housing follows particular thermal constraints in order to reduce parasitic thermal loads (Fig. 4). While the active load (primarily CAMEX) is 0.36W, the total heat load is of the order of 2W per camera. The total amount of <15W at -60°C will allow a passive cooling using radiators and heat-pipes. A temperature control maintains the stability of the CCD-temperature within ± 0.5K. Although we plan for an equatorial orbit, the CCD is shielded by a

massive copper plate on both sides. Fluorescence X-ray radiation generated by cosmic particles is minimized by a graded shield consisting of aluminium and boron carbide. For calibration purposes, each camera housing contains a radioactive Fe^{55} source and an aluminium target providing two spectral lines at 5.9keV (Mn Kα) and 1.5keV (Al Kα). The mechanism for moving the calibration source into and out of the field of view is adopted from an earlier rocket flight experiment. The design of the housing has been finished, and we are now preparing the engineering model.

The experiment electronics, separated in seven electronics boxes has the following tasks:

- A "sequencer" consisting of a FPGA logic provides the correct timing signals for CCD, CAMEX and the two ADC.
- Two 14-bit ADC for each CCD-module digitize the CAMEX output signal.
- The main event processing is performed by a DSP. This comprises the subtraction of an offset-map, the correction of common modes, the application of pixel-wise thresholds using a previously stored noise map, and the delivery of event data frames to the controller.
- A controller, which collects telemetry information (both, events and housekeeping), executes commands, and forms the interface to the S/C.

Since the radiation load in an equatorial orbit is rather low, we plan to use components which are qualified according to MIL883 or the automotive standard.

The complete electronics exists and works already as breadboard model.

The average data rate is determined by the brightness of the extragalactic sky background. We assume to detect between 30 and 40 photons per second (all modules). Since most of the detected photons produce charges in more than one pixel (split-events), and each event is coded using 30 bits, we will have ~ 3.6kbit/s. With some overhead and together with HK data, the data rate will be below 10kbits/s. A bright source (e.g. Cyg X-2) will increase this number to 100kbits/s, for a short time.

Commanding of the eROSITA cameras is simple because only a few operational modes are implemented:

- Standby: camera completely switched off, survival heaters are controlled by S/C.
- Checkout, Test: Electronics switched on, CCD still off.
- Normal: camera is completely switched on and working; this includes also calibration.

2.4 Telescope Structure

The optical bench connects the mirrors system and the baffles on one side with the focal plane instrumentation on the other side. Additionally it forms the mechanical interface to the S/C bus. It has to meet the tough requirements concerning cleanliness, particularly dust. For this reason the telescope contains a front cover which is closed during ground operations and liftoff. The stiffness of the structure requires particular emphasis because of the weight of the telescope is dominated by the mirror system which is far above the S/C structure. The design of the telescope structure is currently investigated by an industrial study.

2.5 Mission profile and Operation

The scientific goals require a variety of mission phases and observing modes, respectively:

- All-sky survey, i.e. a continuous scan with one revolution per orbit
- Extragalactic survey (survey with variable scan speed)
- Deep Survey (pointing mode)
- Pointed observations

In order to keep S/C operations as simple as possible, we will combine the three surveys into a single one with a rotation axis which is tilted with respect to the Sun: a simple geometry having this rotation axis facing towards the Sun (ROSAT, ABRIXAS) would lead to an overlap of all great circles at the ecliptic poles. Tilting the rotation axis towards the galactic plane would automatically give the extragalactic sky a higher exposure with a rather deep exposure closer to the galactic

poles (figures 5 and 6). A tilt of <30° away from the Sun seems to be compatible with other constraints, e.g. the minimum Sun angle. A precession of the rotation axis will distribute smoothly the exposure time over a region of 200 deg^2 around the survey poles.

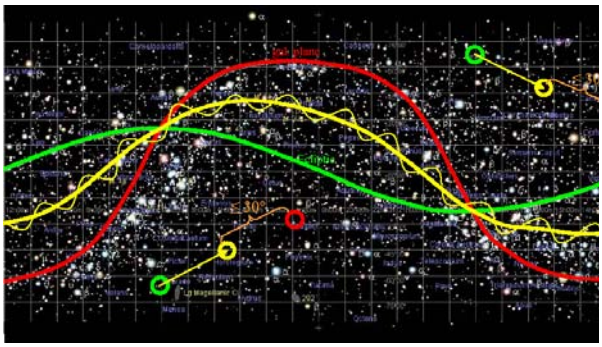

Fig. 5: Galactic equator and poles (red line and circles, respectively) and ecliptic equator and poles (green), and the scan geometry (yellow).

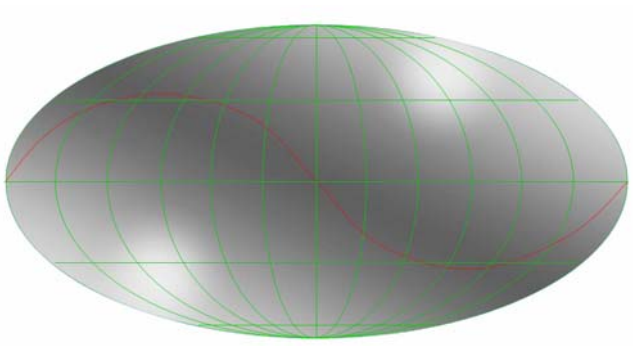

Fig. 6: Exposure map for the scan geometry described in figure 5. The red line represents the galactic plane. The deepest exposure corresponds to the areas where all great circles overlap.

2.6 Sensitivity Calculation

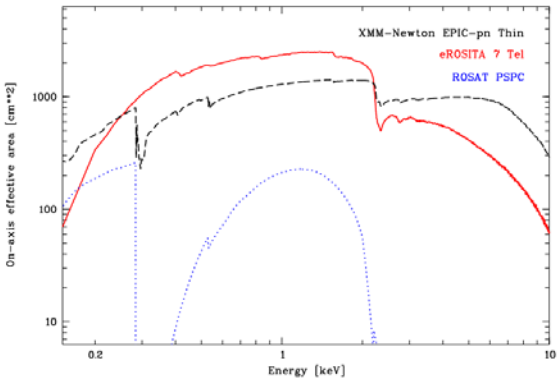

Fig. 7: On-axis effective area of eROSITA (red line) in comparison with one XMM-Newton telescope (black) and the ROSAT-PSPC (blue).

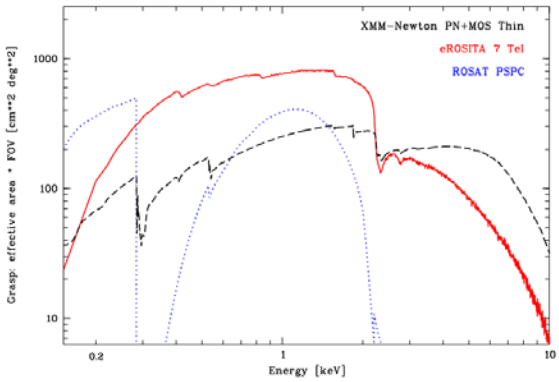

Fig. 8: Grasp of eROSITA (red) in comparison with one XMM-Newton telescope (black) and the ROSAT-PSPC (blue).

Fig. 7 shows the expected on-axis effective area of all seven eROSITA telescopes in comparison with XMM-Newton and ROSAT, Fig. 8 the grasp, i.e. the product of effective area and solid angle of the field of view. The effective area of eROSITA is about twice that of one XMM-Newton telescope in the energy band below 2keV, whereas it is three times less at higher energies. This is a consequence of the small f-ratio (focal length vs. aperture) of the eROSITA mirrors. An advantage of the short focal length is the low instrumental background (per solid angle) and a larger field of view. Since the effective area is split into seven telescopes, also pile-up is less than with a single telescope having comparable area. The eROSITA angular resolution (averaged over the field of view) is better than that of ROSAT due to the smaller field of view and the better spatial resolution of the frame store pn-CCD than that of the ROSAT-PSPC. Furthermore, we will scan for four years (ROSAT 1/2 year). Therefore the eROSITA sensitivity during this all-sky survey will be approximately 30 times ROSAT. When extrapolating from the ROSAT results, we expect to detect 3.2 million AGN and 85,000 clusters of galaxies in the extragalactic sky (see Table 2).

Table 2: Sensitivity calculation for all-sky survey

collecting area (7 Tel., 1.5 keV)	2,471 cm^2
field of view (single telescope)	41 arcmin x 41 arcmin
field of view (total)	0.467 deg^2
mean vignetting	0.70
spatial resolution (detector)	0.075 mm
angular resolution telescope	< 25 arcsec
solid angle all-sky survey	41,253 deg^2
survey duration	4 years
observing efficiency	0.9
exposure time per field of view	1342 s

BKGR countrate, total	16.35 counts/s
BKGR countrate, particles	<0.15 count/s
sensitivity 0.5-2 keV AGN	$9 \cdot 10^{-15}$ erg cm^{-2} s^{-1}
2-10 keV AGN	$1{,}5 \cdot 10^{-13}$ erg cm^{-2} s^{-1}
0.5-2 keV Clusters	$4 \cdot 10^{-14}$ erg cm^{-2} s^{-1}
detected sources:	
0,5-2 keV AGN (10 cts)	3,200,000
2-10 keV AGN (10 cts)	180,000
0,5-2 keV Clusters (50 cts)	86,000

3. SCIENTIFIC GOALS

3.1 Dark Energy

One way to test cosmological models and to asses origin, geometry, and dynamics of our Universe is through the study of the large-scale structure in the matter distribution and its growth with time. Galaxy clusters are ideal tracers of the large-scale structure. The galaxy cluster population provides information on the cosmological parameters in several complementary ways:

1. The cluster mass function in the local Universe mainly depends on the matter density Ω_m and the amplitude of the primordial power spectrum σ_8.
2. The evolution of the mass function f(M,z) is directly determined by the growth of structure in the Universe and therefore gives sensitive constraints on Dark Matter and Dark Energy.
3. The amplitude and shape of the cluster power spectrum, P(k) and its growth with time, depend sensitively on Dark Matter and Dark Energy.
4. Baryonic wiggles due to the acoustic oscillations at the time of recombination are still imprinted on the large scale distribution of clusters and thus can give tight constraints on the curvature of space at different epochs.

The constraints provided by the different cosmological tests with clusters are complementary in such a way, that degeneracies in the parameter constraints in any of the tests can be broken by combinations. The simultaneous constraint of Ω_m and σ_8 by combining method 1 and 3 above is one such example (Schuecker et al. 2003). In addition the combination of several tests provides important consistency checks as explained below. In addition to the above applications, galaxy clusters have been used as cosmological standard candles to probe absolute distances, analogous to the cosmological tests with supernovae type Ia:

- The assumption that the cluster baryon fraction is constant with time combined with observations of this quantity provides constraints on Dark Matter and Dark Energy (e.g. Allen et al. 2004).
- In a very similar way, combined X-ray and Sunyaev-Zeldovich-measurements provide a means for absolute distance measurements and constraints of the geometry of the Universe (e.g. Molnar et al. 2005).

Large, well defined and statistically complete samples of galaxy clusters (which are dynamically well evolved and for which masses are approximately known) are obvious prerequisites for such studies. Substantial progress in the field requires samples of tens to hundreds of thousands of clusters. Surveys in several wavelength regions are used or planned to be used to achieve this goal.

In X-ray surveys, galaxy clusters are detected by the radiation of the hot intracluster medium. X-ray observations are up

to date still the most efficient means to provide cluster samples with these qualities, (i) since X-ray luminosity is tightly correlated to the gravitational mass (Reiprich & Böhringer 2002), (ii) because bright X-ray emission is only observed when the cluster is well evolved showing a very deep gravitational potential well, and (iii) because the X-ray emission is highly peaked, minimizing projection effects. Therefore most cosmological studies involving galaxy clusters are based on X-ray surveys (e.g. Henry 2000, 2004, Böhringer et al. 2000, 2004, Vikhlinin 2003).

3.2 The eROSITA Cluster Survey

The eROSITA flux limit of the survey in the 0.5 to 2 keV band will be about 4×10^{-14} erg s^{-1} cm^{-2} (an order of magnitude deeper than the ROSAT Survey, Fig 9) over most of the sky and about ten times deeper in the poles of the survey scan pattern. At this flux the X-ray sky is dominated by clusters and AGN, which can be separated with an angular resolution of 25". The number–flux relationship is well known to the proposed depth (Gioia et al. 2001; Rosati et al. 2002). The proposed survey will identify ~100,000 clusters. Multi-band optical surveys to provide the required photometric redshifts are already in the planning stages, and will be contemporaneous with or precede the X-ray survey. The cluster population will essentially cover the redshift range z = 0 – 1.5 and will reveal all evolved galaxy clusters with masses above 3.5×10^{14} h^{-1} M_{sun} up to redshifts of 2. Above this mass threshold the tight correlations between X-ray observables and mass allow direct interpretation of the data.

- This sample size is necessary for example to precisely characterize the cluster mass function and power spectrum in at least ten redshift bins, to follow the growth of structure with time.
- to study in detail the biasing of the cluster power spectrum as a function of the cluster mass in order to obtain a better understanding and confirmation of the cluster mass calibration. The biasing describes the ratio of the amplitude of the density fluctuations in the galaxy cluster versus the matter distribution. This parameter can be determined theoretically as a function of mass and the comparison with observations will serve as an important calibration check.

A statistics of at least 50,000 to 100,000 clusters is necessary to reveal the baryonic oscillations in the cluster distribution power spectrum (Angulo et al. 2005).

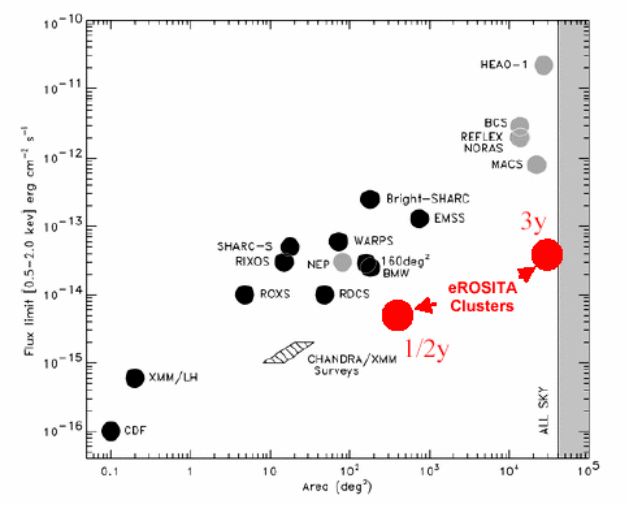

Fig 9: Sensitivity of the eROSITA galaxy cluster survey (red dots) in comparison with previous surveys.

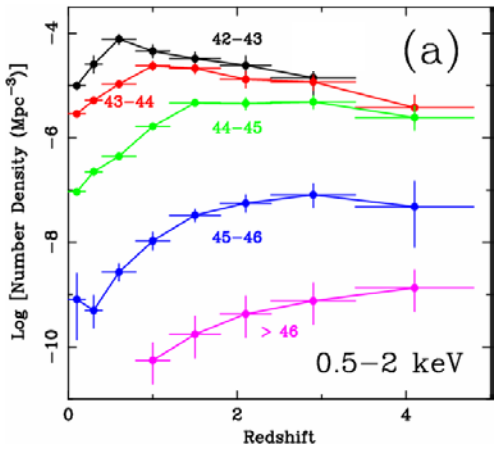

Fig. 10: The luminosity function of AGN shows that low luminosity AGN occur later in the evolution of the Universe than high luminosity quasars.

3.3 Obscured AGN

The detection of all (including obscured) AGN in the local Universe was the primary goal of ABRIXAS and ROSITA before the existence of Dark Energy was realized. This is still one of the main goals of the new eROSITA mission. Deep surveys in the hard X-ray range with Chandra and XMM-Newton, in the mid-infrared with ISO and in the sub-mm with the SCUBA and MAMBO bolometers, together with population synthesis models, have shown that both the cosmic star forming rate and the black hole feeding rate were about two orders of magnitude higher in the early Universe than today (Brandt & Hasinger, 2005, Fig. 10). The decline of this activity occurred at a surprisingly recent stage in cosmic history and is as yet not understood. Many hidden, but still very active black holes should be lurking in rather nearby galaxies, waiting to be detected by a hard X-ray survey.

3.4 Other scientific goals

Among many other interesting science targets are:

- Tidal disruption of a star when approaching a supermassive black hole causes a bright X-ray flare in an otherwise dull galaxy. The decay time of this flare is of the order of years.
- According to the scan geometry, every source in the sky will be seen every half year 10 times in consecutive orbits for about 10 s per orbit. With a sensitivity of 40μCrab per 10 s, the GRB afterglow will be observable for two days. We expect to detect 600 afterglows during the four years of the all-sky survey.
- Large scale diffuse emission: With 30 times better sensitivity and much superior energy resolution, eROSITA will be able to perform detailed spectroscopic studies where ROSAT could yield only a four-band photometry.
- Dust scattering halos have diameters up to several degrees. eROSITA combines the advantage of ROSAT (unlimited field of view) with that of XMM-Newton (energy resolution) and provides, in addition, a substantially reduced pile up which hampers the observation of halos because bright central sources are needed for this kind of studies.

REFERENCES

1. Allen S. W., Schmidt R. W., Ebeling H., Fabian A. C., van Speybroeck, L. " Constraints on dark energy from Chandra observations of the largest relaxed galaxy clusters", MNRAS 353, 457 (2004)
2. Angulo R., Baugh C. M., Frenk C. S., Bower R. G., Jenkins A., Morris S. L. " Constraints on the dark energy equation of state from the imprint of baryons on the power spectrum of clusters", MNRAS, 362, L25 (2005)
3. Böhringer H., Voges W., Huchra J. P., et al.. " The Northern ROSAT All-Sky (NORAS) Galaxy Cluster Survey. I. X-Ray Properties of Clusters Detected as Extended X-Ray Sources" ApJS 129, 435 (2000)
4. Böhringer H., Schuecker P., Guzzo, L, et al., " The ROSAT-ESO Flux Limited X-ray (REFLEX) Galaxy cluster survey. V. The cluster catalogue" A&A 425, 367 (2004)
5. Brandt N., Hasinger G., " Deep Extragalactic X-Ray Surveys", ARA&A 43, 827 (2005)
6. Fraser G., Brunton A., Bannister N et al., "LOBSTER-ISS: an imaging x-ray all-sky monitot for the International Space Station", at. Proc. SPIE 4497, 115-126, X-ray and Gamma-Ray Instrumentation for Astronomy XII, Kathryn A. Flanagan, Oswald H. Siegmund, Eds. (2002)
7. Friedrich P., Predehl P., Meidinger N., Strüder L., Vongehr M., Burkert W., Freyberg M., Hartner G., Bräuninger H., Hasinger G., Hofer S., Stuffler T., Hagl F., Hollerith C. " Results from a contamination experiment on the ISS", at Proc. SPIE 5900, N-1 – N-12, Optics for EUV, X-Ray, and Gamma-Ray-Astronomy II, edit. by Oberto Citterio, Stephen L. O'Dell (2005).
8. Gioia I. M., Henry J. P., Mullis C. R., Voges W., Briel U. G., Böhringer H., Huchra, " Cluster Evolution in the ROSAT North Ecliptic Pole Survey", ApJ 533, 105 (2001)
9. Haiman et al., 2005 astro-ph/0507013
10. Henry, P., " Measuring Cosmological Parameters from the Evolution of Cluster X-Ray Temperatures", ApJ 534, 565 (2000)
11. Henry, P., " X-Ray Temperatures for the Extended Medium-Sensitivity Survey High-Redshift Cluster Sample: Constraints on Cosmology and the Dark Energy Equation of State", ApJ 609, 603 (2004)

12. Meidinger N., Hartmann R., Holl P., Hyder E., Hasinger G., Herrmann S., Strüder, L. "Systematic testing and results of x-ray CCDs developed for eROSITA and other applications", Proc. SPIE 6276, Eds. David A. Dorn, Andrew D. Holland (2005)
13. Pavlinsky M., Hasinger G., Parmar A., Fraser G., Churazov E., Gilfanov M., Sunyaev R., Vikhlinin A., Predehl P., Piro L., Arefiev V., Tkachenko A., Pinchuk V., Grobets D. "Spectrum-RG/eROSITA/Lobster astrophysical mission", Proc. SPIE 6266, Eds. Martin J.L. Turner, Günther Hasinger (2005)
14. Pfeffermann E., Bonerz S., Bräuninger H. et al. "Concept of the ROSITA x-ray camera", X-ray and Gamma-ray Telescopes and Instruments for Astronomy. Edited by Jachim E. Trümper, Harvey D. Tananbaum. Proc SPIE 4851, 749-856 (2003)
15. Predehl, P., Friedrich, P., Hasinger, G., "ROSITA: scientific goal and mission concept", at X-ray and Gamma-Ray Telescope and Instruments for Astronomy. Edited by Joachim Trümper, Harvey D. Tananbaum. Proceedings of the SPIE 4851, 314-323 (2003)
16. Predehl P. "ABRIXAS: scientific gal and mission concept", Proc SPIE 3765, 172-183, EUV, X-ray, and Gamma-ray Instrumentation for Astronomy X, Oswald H. Siegmund, Kathryn A. Flanagan, Eds (1999)
17. Reiprich, T., Böhringer, H., 2002, ApJ 567, 716
18. Rosati P, Borgani S, Norman C, " The Evolution of X-ray Clusters of Galaxies", ARA&A 40, 539 (2002)
19. Schuecker P., Böhringer H., Collins C. A., Guzzo L., "The REFLEX galaxy cluster survey. VII. $Omega_m$ and $sigma_8$ from cluster abundance and large-scale clustering", A&A 398, 867 (2003)
20. Vikhlinin A., Voevodkin A., Mullis C. R., VanSpeybroeck L., Quintana H., McNamara B. R., Gioia I., Hornstrup A., Henry J. P., Forman W. R., Jones C., " Cosmological Constraints from the Evolution of the Cluster Baryon Mass Function at z ~ 0.5", ApJ 590, 15 (2003)